Flow and heat transfer in a rotating cylindrical cavity with a radial inflow of fluid

Part 2: Velocity, pressure and heat transfer measurements

M. Firouzian, J. M. Owen, J. R. Pincombe and R. H. Rogers*

Velocity, pressure and heat transfer measurements have been made inside a rotating cavity with a radial inflow of fluid for a wide range of flow rates and rotational speeds. The air-filled cavity comprised two discs and a peripheral shroud; five different perforated and slotted shrouds were used to test the effect of inlet geometry. The tangential component of velocity was measured, in the source region and in the interior core between the Ekman layers, using a laser-doppler anemometer. For the outer part of the source region, the data were consistent with free vortex flow; for the interior core, the data were, in the main, in good agreement with existing nonlinear laminar and turbulent Ekman layer theory. Pressure measurements, made for only one of the six shrouds, were in reasonable agreement with a simple theoretical model. Under some conditions, radial pressure drops of magnitude over twenty times that associated with solid-body rotation were measured and predicted. Heat transfer measurements were made with one of the discs heated. The variations in the magnitude of the Nusselt numbers on the hot disc were consistent with the hole geometry in the shrouds. For similar conditions, the magnitudes compared with those reported for radial outflow tests.

Keywords: *fluid flow, heat transfer, rotating cavity, rotating discs*

In Part 1 of this work[1] the flow structure of a rotating cylindrical cavity with a radial inflow of fluid was studied. A simple model of the flow inside the source region was used to estimate the extent of this region, and flow visualization was used to study the flow structure and to obtain measurements of the size of the source region.

In Part 2, experimental measurements of the tangential component of velocity, the radial pressure drop and the Nusselt numbers are presented. The apparatus is described and measured velocity distributions are compared with values obtained from solutions of the linear and nonlinear Ekman layer equations using momentum-integral techniques[2]. Theoretical estimates of the pressure coefficient are compared with measurements, and the measured values of the Nusselt numbers are discussed.

The experimental apparatus

The rig used for the velocity, pressure and heat transfer experiments is described in Part 1.

The tangential component of velocity inside the cavity was measured by laster-doppler anemometry (LDA). The system comprised transmitting and receiving optics arranged in the backscatter real-fringe mode. For the transmitting optics, a Spectra Physics argon-ion laser (operating in the single-line mode of 514 nm at an output power of approximately 150 mW) was used with a 50–50 beam splitter, which produced a separation distance of 30 mm, and a 300 mm focal length convex lens. This arrangement produced a nominal optical probe volume of 0.16 mm diameter, 3.28 mm length, with a fringe spacing of 5 μm. The optics were mounted on a traversing table that enabled the probe volume to be moved in a radial direction. All velocity measurements were made with the probe volume in, or near, the mid-axial plane ($z/s = 0.5$) of the cavity.

The backscattered light from the probe volume was steered by a mirror through a receiving lens and pinhole to a photomultiplier. The signal from the latter was processed by a Cambridge Consultants tracking filter. The tracking filter, which could accept doppler frequencies up to 15 MHz, produced an analogue voltage proportional to the doppler frequency. The true time-average of this voltage, which was proportional to the time-average velocity, was obtained from a Solartron Time-Domain Analyzer.

The seeding for the LDA tests was achieved by a Norgren 'micro-fog lubricator', which generated oil particles of approximately 2 μm diameter. As for the flow visualization, the air immediately outside the cavity was seeded with these particles, which were then drawn into the cavity along with the cooling air. Further details of the optical instrumentation are given by Pincombe[3].

* School of Engineering and Applied Sciences, University of Sussex, Falmer, Brighton, Sussex, UK
Received 10 October 1984 and accepted for publication in final form on 13 May 1985

The velocity distribution

Figs 1 to 4 show the radial variation of tangential velocity for shrouds A, B, E and F, respectively; no velocity measurements were made with shrouds C and D. 'Free vortex' and 'linear theory' refer to Eqs (1) and (2), respectively, or Part 1. The 'non linear theory'[2] was started with $V_\phi/\Omega r = 1$ at $x = c^{1/2}$, where c is the empirically-determined swirl fraction of the incoming fluid; according to the linear theory in Part 1, this value of x denotes the limit of reverse flow in the source region.

In Part 1 the radial extent of the source region was correlated, for shrouds A to D, using a swirl fraction of $c = 0.54$ for laminar flow and $c = 0.59$ for turbulent flow. For the curves shown in Figs 1 and 2, a value of $c = 0.59$ was used for both laminar and turbulent flow. The intercept of the free vortex curve and the 'linear theory' curve mark the approximate edge of the source region.

Fig 1 shows the variation of $V_\phi/\Omega r$ with x for (a) laminar flow ($Re_r < 180$) and (b) turbulent flow ($Re_r > 180$) when shroud A (the 'central-inlet' shroud) is used. In Fig 1a the non linear laminar curves are in good agreement with the data for $Re_\phi/10^5 = 1.97$ and 4; for $Re_\phi/10^5 = 6$, the non linear curve is slightly higher than the measured velocities. The non linear turbulent curves in Fig 1b are in good agreement with the measured velocities for all three values of Re_ϕ.

Fig 2 shows similar results for shroud B (the 'twin-inlet' shroud). Again, the agreement between the non-linear curves and the experimental data is good, with the exception of the turbulent results, in Fig 2b, for $Re_\phi/10^5 = 0.985$.

Fig 3 shows the velocity distribution for shroud E (the 'slotted-inlet' shroud). No flow visualization was carried out to measure the extent of the source region for this shroud; however, a value of $c = 0.42$ provided a reasonable fit to the data, most of which are believed to be in the source region.

Fig 4 shows the radial variation of tangential velocity for shroud F (the 'foam-filled shroud'). For this shroud, the fluid was assumed to enter the cavity with solid-body rotation (a contention that was supported by the measurements of the size of the source region in Part 1); the swirl fraction c was accordingly chosen to be unity.

The results shown in Fig 4a for laminar flow are, in the main, in good agreement with the non linear curves. In Fig 4b, the agreement between the measured velocities and the turbulent non linear curves is also reasonable. The source region for shroud F is much smaller than that of the other shrouds, and most of the data are in the interior core.

The pressure drop across the cavity

Theoretical estimate of the pressure drop

In regions where viscous effects are negligible and where the radial and axial components of velocity are small

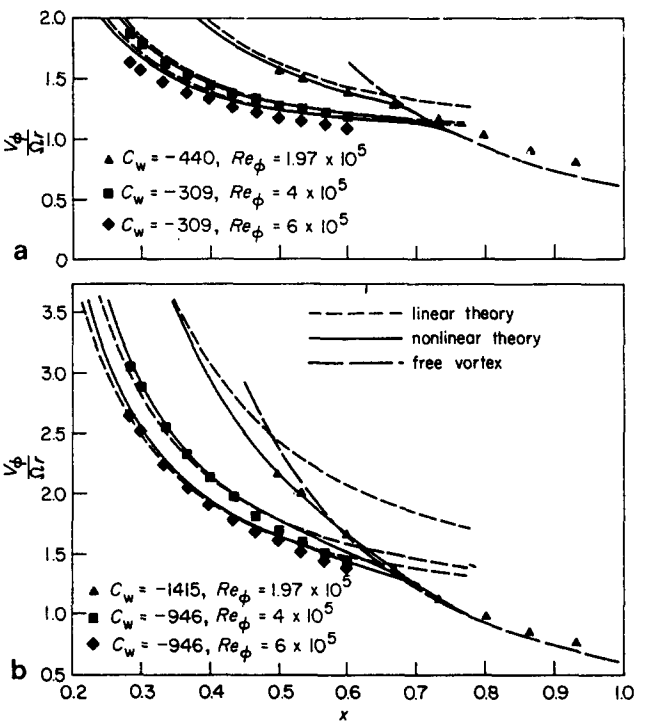

Fig 1 Variation of tangential component of velocity with radius for isothermal flow (shroud A): (a) $Re_r < 180$, laminar theory; (b) $Re_r > 180$, turbulent theory

Notation

a	Inner radius of disc
b	Outer radius of disc
c	Inlet swirl fraction
C_p	Pressure coefficient $= \Delta p/\frac{1}{2}\rho\Omega^2 b^2$
C_w	Flow rate coefficient $= Q/\nu b$
k	Thermal conductivity
Nu_{av}	Average Nusselt number $= q_{av} b/k(T_s - T_I)_{av}$
p	Pressure
q	Heat flux
Q	Volumetric flow rate
r	Radial coordinate
r_e	Radius of edge of source region
Re_r	Radial Reynolds number $= C_w/2\pi x$
Re_ϕ	Rotational Reynolds number $= \Omega b^2/\nu$
s	Axial spacing between rotating discs
T	Temperature
V_ϕ	Tangential component of velocity relative to a stationary reference frame
x	Dimensionless radial coordinate $= r/b$
x_a	Dimensionless inner radius $= a/b$
x_e	Dimensionless radius of edge of source region $= r_e/b$
z	Axial coordinate
Δp	Pressure drop from $x = 1$ to $x = x_a$
λ	$= \lambda_L$ or λ_T for laminar or turbulent Ekman-layer flow
λ_L	$= (1/2\pi) C_w Re_\phi^{-1/2}$
λ_T	$= \mathrm{sgn}(Q) 2.22 \lvert C_w \rvert^{9/8} Re_\phi^{-1/2}$
ν	Kinematic viscosity
ρ	Density
Ω	Angular speed of cavity

Subscripts

av	Radially-weighted average value
I	Pertaining to conditions at inlet to cavity
s	Pertaining to cavity-side surface of heated disc

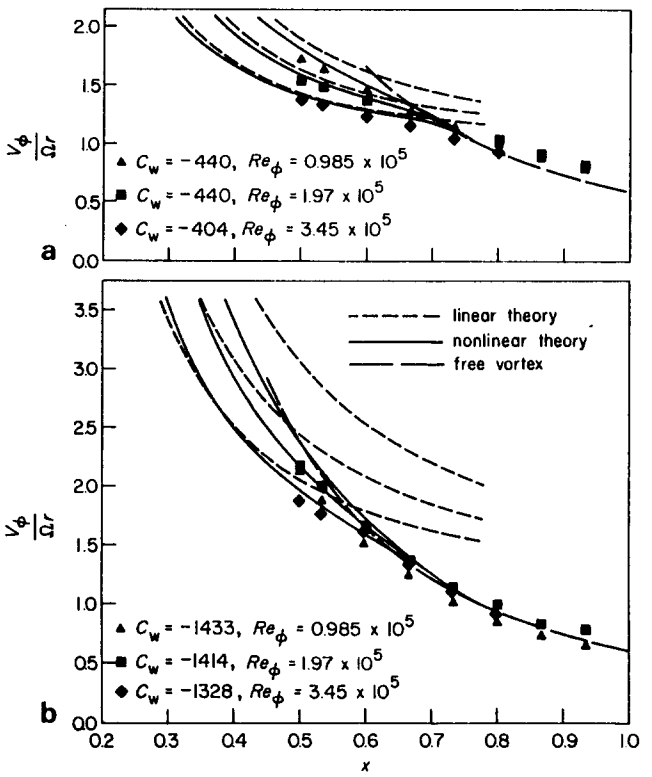

Fig 2 Variation of tangential component of velocity with radius for isothermal flow (shroud B): (a) $Re_r < 180$, laminar theory; (b) $Re_r > 180$, turbulent theory

compared with the tangential component, V_ϕ, the radial pressure gradient can be calculated from

$$\frac{1}{\rho}\frac{dp}{dr} = \frac{V_\phi^2}{r} \tag{1}$$

This equation is valid, away from the Ekman layers, for the source region and for the interior core; and, if the sink layer is ignored, it can be used to calculate the pressure drop, Δp, that occurs as the fluid moves from the source at $x=1$ to the sink at $x=x_a$. Hence, using the definition of the pressure coefficient C_p given in the Notation, and assuming incompressible flow, Eq (1) can be written in the integral form

$$C_p = 2\int_{x_a}^{1} x(V_\phi/\Omega r)^2\,dx \tag{2}$$

Eq (2) can be integrated if $V_\phi/\Omega r$ is known; for simplicity, Eqs (1) and (2) of Part 1 are used. This assumes that the flow outside the boundary layers in the source region is a free vortex, and that the boundary layers elsewhere are Ekman layers. Hence, for laminar Ekman-layer flow,

$$C_p = (x_e^2 - x_a^2) + 4|\lambda_L|\ln(x_e/x_a) + \lambda_L^2(x_a^{-2} - x_e^{-2}) + c^2(x_e^{-2} - 1) \tag{3}$$

where x_e is calculated from Eq (5) of Part 1. For turbulent flow,

$$C_p = (x_e^2 - x_a^2) + \frac{32}{3}|\lambda_T|(x_e^{3/8} - x_a^{3/8}) + \frac{8}{5}\lambda_T^2(x_a^{-5/4} - x_e^{-5/4}) + c^2(x_e^{-2} - 1) \tag{4}$$

where x_e is calculated from Eq (6) of Part 1.

These equations are only valid for $|\lambda| < c$ (that is, for $x_e > x_a$, such that the source region does not fill the entire cavity). For $|\lambda| \geq c$ (that is, for the case where the source region does fill the cavity), free vortex flow is assumed to occur throughout, and

$$C_p = c^2(x_a^{-2} - 1) \tag{5}$$

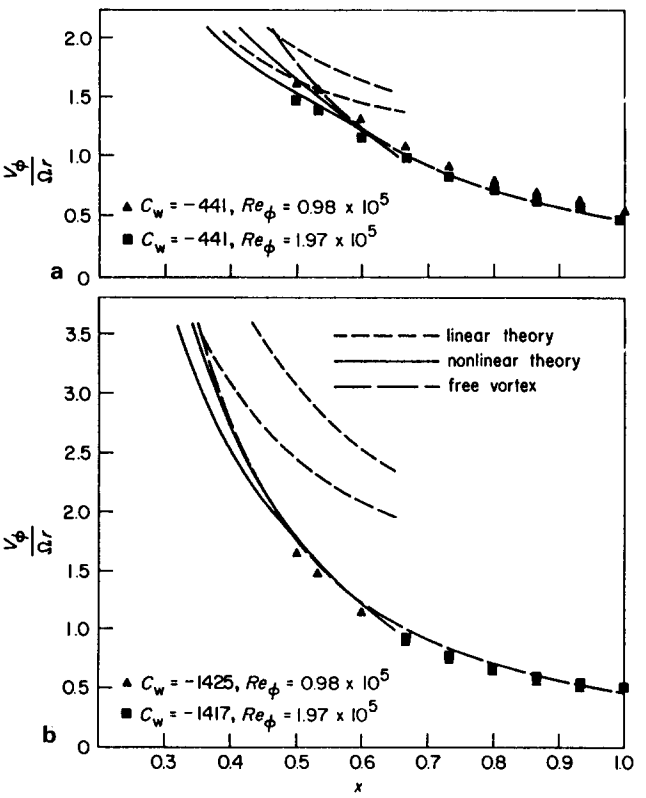

Fig 3 Variation of tangential component of velocity with radius for isothermal flow (shroud E): (a) $Re_r < 180$, laminar theory; (b) $Re_r > 180$, turbulent theory

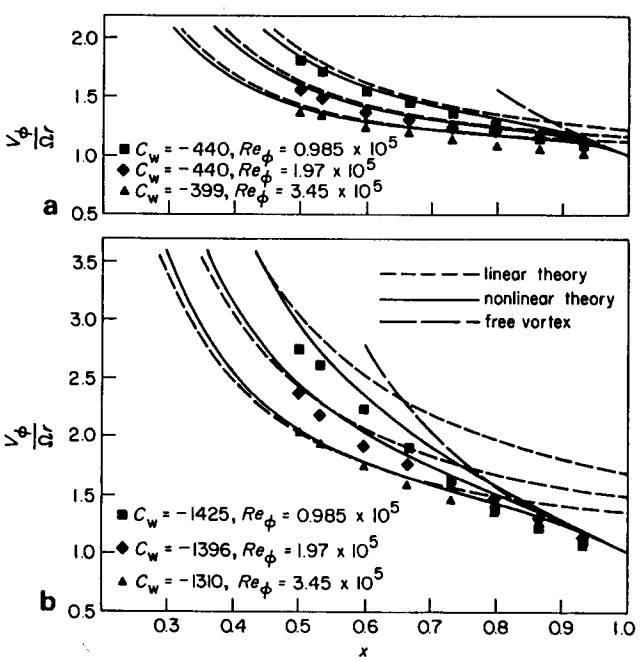

Fig 4 Variation of tangential component of velocity with radius for isothermal flow (shroud F): (a) $Re_r < 180$, laminar theory; (b) $Re_r > 180$, turbulent theory

For the limiting case of zero flow rate ($\lambda = 0$), $x_e = c^{1/2}$, and Eqs (3) and (4) both reduce to

$$C_p = c(2-c) - x_a^2 \qquad (6)$$

For all practical cases, Eqs (5) and (6) provide the upper and lower bounds, respectively, for the pressure drop in the cavity. Using Eqs (3) and (4), the calculated variation of C_p with $|\lambda_L|$ and $|\lambda_T|$ is shown in Fig 5 for $0.1 \leqslant c \leqslant 1$ and $x_a = 0.1$. It should be noted that these equations do not include the 'inlet loss' (the pressure drop that occurs as the fluid passes through the holes in the shroud) or the 'exit loss' (that occurs as the fluid leaves the cavity); these losses can be determined empirically, as discussed below.

Pressure measurements

As described in Part 1, the radial pressure drop across the cavity was measured using a static pressure tap on the stationary piping downstream of the cavity. This measurement represented the overall pressure drop, relative to atmospheric pressure outside the cavity, and included the pressure 'losses' across: (i) the shroud itself; (ii) the cavity; (iii) the exit from the cavity to the stationary piping. The inlet loss (i) and exit loss (iii) must be found empirically, but the pressure drop across the cavity can be calculated as described above.

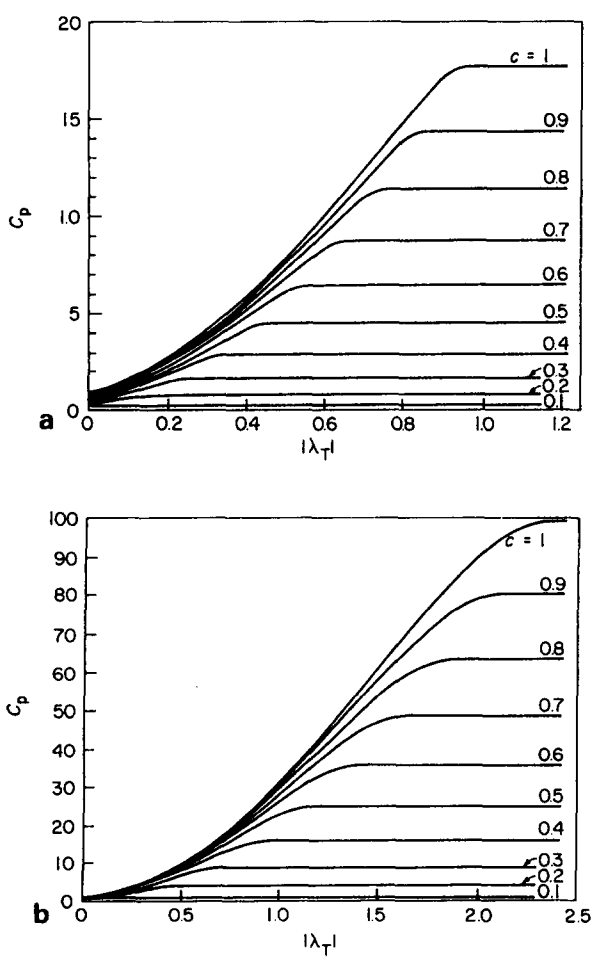

Fig 5 The effect of the swirl fraction, c, on the variation of C_p with (a) $|\lambda_L|$ and (b) $|\lambda_T|$ according to Eqs (3) and (4) with $x_a = 0.1$

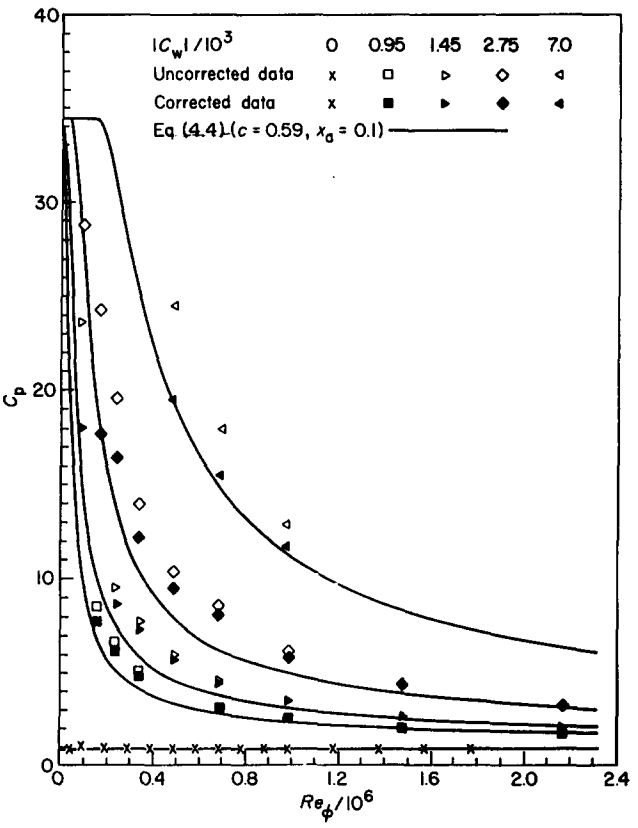

Fig 6 The variation of C_p with Re_ϕ for shroud A

The inlet and exit losses were determined, for shroud A, by measuring the overall pressure drop when the cavity was stationary; no estimates were practicable when the cavity was rotating. It should also be pointed out that most of the pressure measurements were made during the heat transfer experiments: a separate programme of pressure measurements was not conducted. For this reason, and owing to the difficulties in estimating the inlet and exit losses, the measurements were subject to indeterminate errors. Although tests were made with a number of the shrouds, only the results for shroud A (for which data were available to estimate the inlet and exit losses) are presented below.

Fig 6 shows the variation of C_p with Re_ϕ for $0 \leqslant |C_w| \leqslant 7000$. The 'uncorrected data' are based on the measured pressure drop, and the estimated inlet and exit losses have been subtracted from these to produce the 'corrected data'. The theoretical curves are based on Eq (4) with $x_a = 0.1$ and $c = 0.59$, which is the value for the swirl fraction that was used above. Bearing in mind the experimental difficulties, agreement between the corrected data and the theoretical curves is good. For $C_w = 0$, Eq (4) reduces to $C_p = 0.82$; the experimental data are correlated by $C_p = 0.83$.

Fig 7 shows the variation of C_p with C_w for $0.25 \leqslant Re_\phi/10^6 \leqslant 2.2$; only corrected data are shown, and the theoretical curves are again based on Eq (4) with $x_a = 0.1$ and $c = 0.59$. The agreement between the measured and calculated values is reasonable, although there is a tendency for the theoretical curves to underestimate the data at the lower values of Re_ϕ. It is of some interest, and some design significance, that pressure coefficients as much as twenty times the 'solid-body-rotation' value ($C_p = 1$) have been measured and predicted.

Heat transfer measurements

Experimental technique

The thermocouple readings on the front (cooled) and back (heated) faces of the heated disc were used as boundary conditions for the numerical solution of Laplace's equation. Assuming an axisymmetric temperature distribution, the interior temperature of the disc and the surface heat flux, q, were computed as described by Owen and Bilimoria[4] and Owen and Onur[5]. The average Nusselt number, Nu_{av}, was then calculated from

$$Nu_{av} = q_{av} b / k(T_s - T_I)_{av} \tag{7}$$

where k is the thermal conductivity of the air, T_s is the surface temperature of the front (cavity-side) face of the disc, T_I is the coolant inlet temperature, and 'av' refers to the radially-weighted average value.

It should be noted that q is taken to be positive when the heat flows from the disc into the cooling air. Under some conditions, it is possible for q to be negative even when $(T_s - T_I)$ is positive; this occurs when the cooling air, which flows radially inward, becomes heated to a temperature greater than that of the disc. Fig 8 shows typical radial temperature profiles for the heated disc, and the crossover of the front and back face temperatures at $x \simeq 0.5$ illustrates the effect referred to above. For smaller radii, where q is negative, the local Nusselt numbers are also negative.

The coolant inlet temperature, T_I, was determined from an axial traverse. The temperature probe was located outside the cavity, on the rotational axis, at a radial distance of 11 mm from the shroud; it was traversed over the axial width of the holes in the shroud. The outer faces of the rotating discs acted as free discs, and their boundary layers flowed radially outward on each side of the shroud. As a consequence, hot air from the back (outer) face of the heated disc could be entrained into the cooling air entering the cavity. At the higher rotational speeds, where this 'free disc pumping' was significant, the inlet temperature of the cooling air could be as much as 7°C higher than the ambient temperature, which was approximately 25°C. For all the tests, the maximum disc temperature was approximately 100°C, and this maximum occurred at $x \simeq 0.8$.

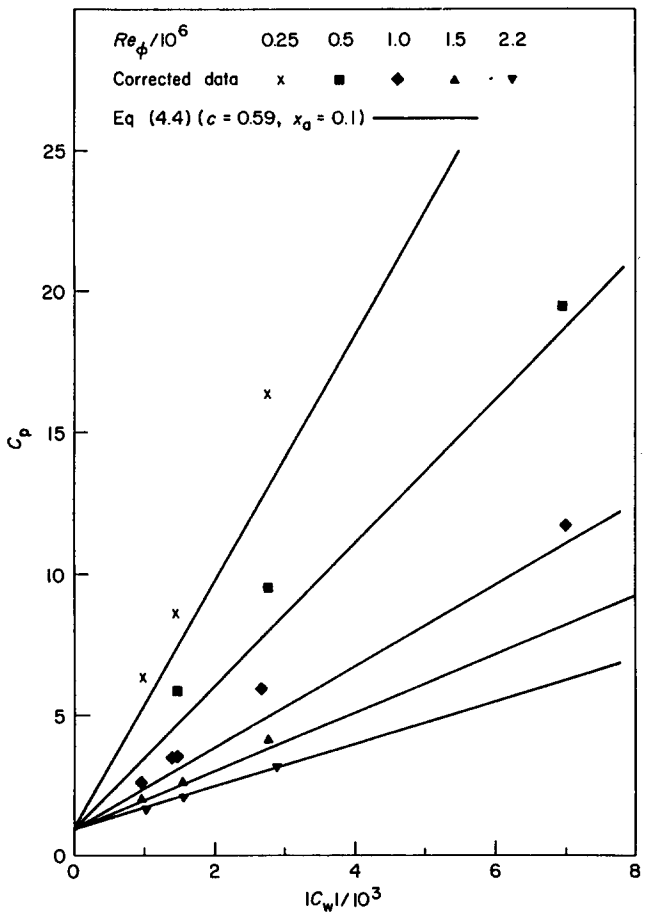

Fig 7 The measured (corrected) variation of C_p with $|C_w|$ for shroud A

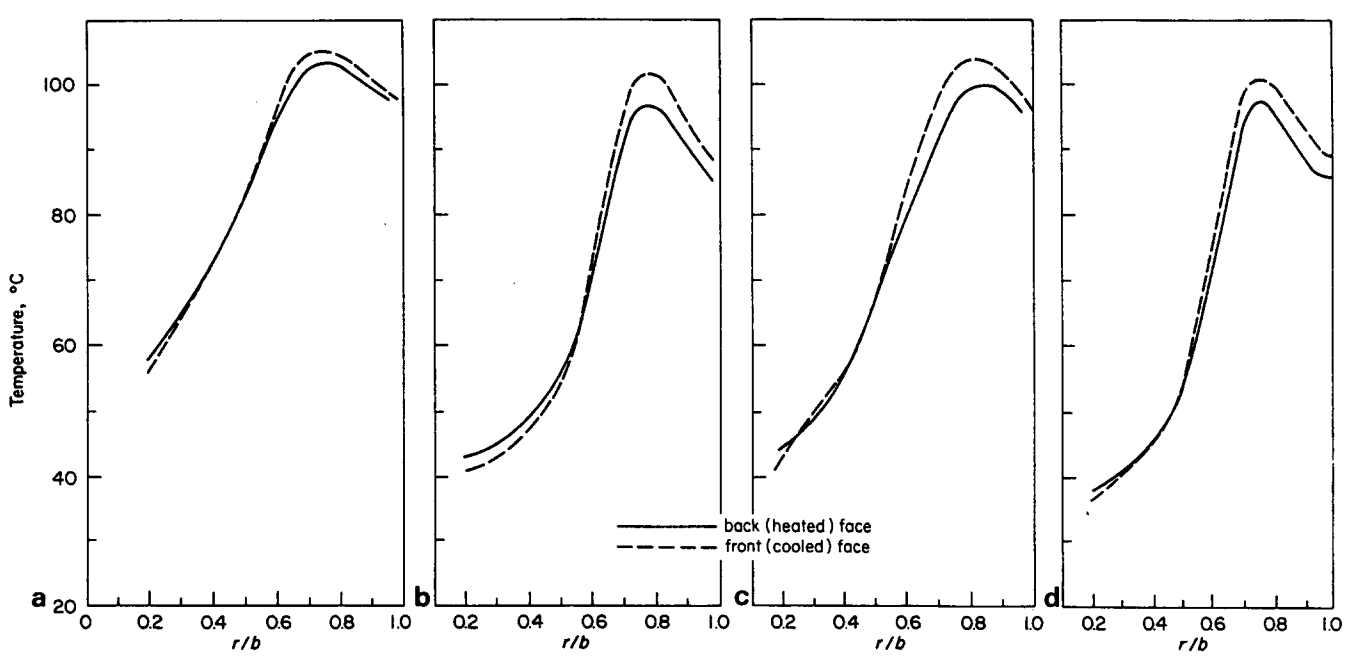

Fig 8 Typical temperature distributions on the heated disc of the rotating cavity: (a) $|C_w| = 2.8 \times 10^3$, $Re = 2.3 \times 10^4$; (b) $|C_w| = 2.8 \times 10^3$, $Re_\phi = 2.1 \times 10^6$; (c) $|C_w| = 2.8 \times 10^4$, $Re_\phi = 2.2 \times 10^4$; (d) $|C_w| = 2.8 \times 10^4$, $Re_\phi = 4.7 \times 10^5$

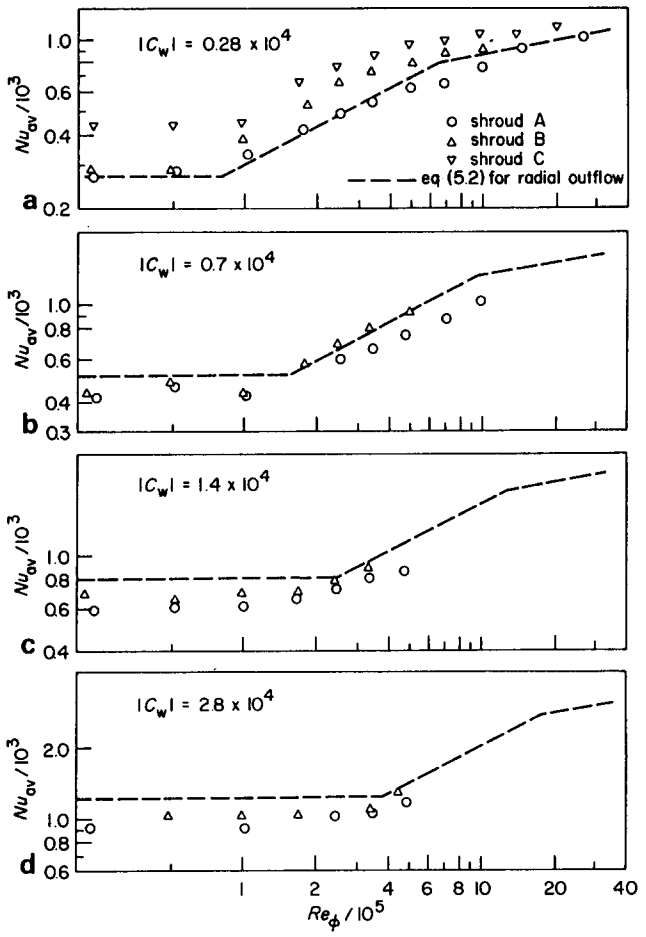

Fig 9 The effect of shroud hole-geometry on the average Nusselt numbers for radial inflow

Average Nusselt numbers

For radial outflow (using a cavity with one disc heated and a 'central-inlet shroud' similar to shroud A), Owen and Onur correlated their turbulent forced convection data in three regimes:

$$\text{Regime I:} \quad Nu_{av} = 1.94 C_w^{2/3} G^{1/6} \tag{8a}$$

$$\text{Regime II:} \quad Nu_{av} = 0.07 Re_\phi^{1/2} C_w^{1/3} \tag{8b}$$

$$\text{Regime III:} \quad Nu_{av} = 4.11 Re_\phi^{1/9} C_w^{1/2} G^{1/9} \tag{8c}$$

The boundaries between the three regimes were delineated by the intercepts of the curves defined by Eqs (8a–c). Regime I is associated with flows in which the source region fills the entire cavity; Regimes II and III are associated with Ekman layer flow. It should be noted that the above correlations, which are for the heated disc, were obtained using a rig virtually identical to that used for the experiments reported here.

Fig 9 shows the variation of Nu_{av} with Re_ϕ for radial inflow, with shrouds A, B and C, for $0.28 \leqslant |C_w|/10^4 \leqslant 2.8$ (and $G = 0.133$); also shown is the correlation for radial outflow given by Eq (8). As $Re_r > 180$ over the entire surface of the disc if $|C_w| > 1130$, the flow should be turbulent for the range of C_w tested.

Referring to Fig 9a, it can be seen that the data for shroud A are close to the outflow correlation. The average Nusselt numbers for shroud C (the 'side-inlet' shroud) are higher than those for shroud B (the 'twin-inlet' shroud); both sets of data are higher than those for shroud A. This is not unexpected: for shroud A, all the coolant enters near the mid-axial plane of the cavity; for shroud B, half the coolant enters adjacent to the hot disc; for shroud C, all the coolant enters adjacent to the hot disc.

No data are available for shroud C at the higher values of $|C_w|$, but Figs 9b, c and d for shrouds A and B show a similar relationship to that described above, although the differences between the results for the two shrouds are smaller. For $|C_w| > 0.7 \times 10^4$, the average Nusselt numbers for radial inflow tend to be lower than the outflow correlations.

Conclusions

Measurements of the velocity, pressure drop and heat transfer have been made inside a rotating cavity with a radial inflow of coolant. Experiments were conducted in a cavity with an axial gap to outer radius ratio of $s/b = 0.133$ and an inner to outer radius ratio of $a/b = 0.1$; five different perforated and slotted shrouds were used to test the effect of inlet geometry.

The tangential component of velocity was measured, using a laser-doppler anemometer, for $400 < |C_w| < 1500$ and $10^5 < Re_\phi < 6 \times 10^5$. For the outer part of the source region, the experimental data were consistent with free vortex flow. The swirl fraction, c, imparted to the fluid at entrance to the cavity, depended on whether the shroud had a series of holes (that is, the shroud was 'perforated'), an open slot or a foam-filled slot: for the first two cases, $c < 1$; for the latter case, $c = 1$. The experimental data in the interior core were, in the main, in good agreement with the nonlinear laminar and turbulent Ekman-layer theory. For the cases where the source region filled all, or most, of the cavity, the nonlinear theory tended to overestimate the measured tangential component of velocity.

A theoretical estimate of the radial pressure drop inside the cavity has been made by using the linear Ekman layer model described in Part 1. Pressure measurements were made for one of the perforated shrouds with $0 \leqslant |C_w| < 7000$ and $0.1 < Re_\phi/10^6 < 2$. The corrected pressure coefficients (in which the estimated inlet and exit losses were subtracted from the total measured pressure drop) were in reasonable agreement with the theoretical values. Under some conditions, pressure drops of magnitude as much as twenty times those associated with solid-body rotation were measured and predicted.

Average Nusselt numbers were measured, for the case when one disc in the cavity was heated, for $2800 < |C_w| < 28\,000$ and $2 \times 10^4 < Re_\phi < 2 \times 10^6$. Tests were conducted using each of the three perforated shrouds, and the variations in the magnitude of the Nusselt numbers were consistent with the hole geometry in the shroud. For similar conditions, the magnitudes of the average Nusselt numbers were similar to those reported for radial outflow tests.

Acknowledgements

The authors wish to thank Motoren- und Turbinen-Union, Rolls Royce Limited and the Science and

Engineering Research Council for supporting the work described in this two-part paper.

References

1. **Firouzian M., Owen J. M., Pincombe J. R. and Rogers R. H.** Flow and heat transfer in a rotating cavity with a radial inflow of fluid. Part 1: The flow structure. *Int. J. Heat and Fluid Flow, 1985*, **6**, *228*
2. **Owen J. M., Pincombe J. R. and Rogers R. H.** Source-sink flow inside a rotating cavity. *J. Fluid Mech., 1985*, **155**, *233*
3. **Pincombe J. R.** *Optical measurements of the flow inside a rotating cylinder. D Phil thesis, 1983, University of Sussex, UK*
4. **Owen J. M. and Bilimoria E. D.** Heat transfer in rotating cylindrical cavities. *J. Mech. Engng Sci., 1977*, **19**, *175*
5. **Owen J. M. and Onur H. S.** Convective heat transfer in a rotating cylindrical cavity. *J. Engng Power, 1983*, **105**, *178*

BOOK REVIEW

Computational Fluid Mechanics and Heat Transfer

D. A. Anderson, J. C. Tannehill and R. H. Pletcher

The book was written in a textbook format based on course notes used in an advance level and graduate course at Iowa State University. In an introductory section a brief review of the physical significance and the mathematical behaviour of the most common partial differential equations encountered in fluid mechanics and heat transfer is presented, followed by the introduction of the basic fundamentals of finite difference techniques. These techniques are then applied to obtain the solution of selected model equations (wave, conduction, Laplace and Burgers). The individual characteristics of the various schemes are illustrated and discussed.

The remainder of the book is devoted to specific applications. A detailed discussion of the appropriate differential equations including those associated with turbulent flows, is followed by a detailed study of the numerical solutions of the equations associated with invicid flow, boundary layer, 'parabolized' Navier Stokes and the complete Navier Stokes equations. The last topic discussed is grid generation.

The treatment of the fundamentals and the application of finite difference techniques in fluid mechanics and heat transfer is well organized and masterfully presented. No generalized programs are presented, but the reader is given all the information he needs to formulate his own program or gain a more complete understanding of an existing algorithm. This book will make a valuable addition to the library of those involved in CFD activities.

Frank W. Schmidt
Department of Mechanical Engineering,
Pennsylvania State University,
PA, USA

Published, price $125.00, by Hemisphere Publishing Corporation, 79 Madison Ave, New York, NY 10016, USA, 1181 pp.

Natural Convection

S. Kakac, W. Aung and R. Viskanta

Buoyant forces play a very important role in a large number of flows found in our environment and in engineering applications. While we have made considerable progress since 1960 in our understanding of these flows, this information has not been collected and documented in a well organized presentation of the subject. It is also recognized that our knowledge of a number of the phenomena involved is so limited that accurate predictions of the rate of heat transfer and details of the flow can not be made at the present time.

In recognition of the importance of natural convection a NATO Advanced Study Institute was held in 1984 to disseminate current information and highlight areas in which there is a critical need for further study. This book is composed of lectures and papers presented at the Advanced Study Institute.

Specific topics discussed include: external boundary layer flows; plane layers; flows in enclosures and in the presence of a stratified fluid; natural convection in porous media and in melting and solidification; and mixed convection. Specific emphasis is also placed upon turbulence modelling and the influence of temperature dependent properties.

Like many proceeding volumes there is an unevenness in the treatment of some of the topics. Of particular interest are the contributions dealing with turbulence modelling, mixed convection, natural convection in melting and solidification process and the summary article dealing with still unsolved problems in natural convection. The editors are to be congratulated for assembling an extremely useful book for those interested in buoyant driven flows.

Frank W. Schmidt
Department of Mechanical Engineering,
Pennsylvania State University,
PA, USA

Published, price $39.95, by Hemisphere Publishing Corporation, 79 Madison Ave, New York, NY 10016, USA, 599 pp.